Оригинальная статья

UDC: 669.018.95

DOI: 10.57070/2304-4497-2023-1(43)-24-32

A COMPARATIVE STUDY ON NICKEL-BASED ALLOY COMPOSITE CLADDINGS PREPARED BY TUNGSTEN INERT GAS AND MICROWAVE HYBRID HEATING TECHNIQUES

© 2023 S. Gudala[1], S. Konovalov[1], M. R. Ramesh[2], I. Panchenko[1]

[1]**Siberian State Industrial University** (42 Kirova Str., Novokuznetsk, Kemerovo Region – Kuzbass, 654007, Russian Federation)

[2]**National Institute of Technology Karnataka** (NH 66, Srinivasnagar, Surathkal, Mangalore, Karnataka, 575025, India)

Abstract. In this study, tungsten inert gas (TIG) and microwave hybrid heating (MHH) cladding techniques are used to develop thick nickel-based alloy clad layers of 1mm thickness on a titanium 31 alloy substrate. In TIG cladding consider current was considered as a process variable, whereas in MHH cladding, exposure time was considered as the process variable. Scanning electron microscopy (SEM) with energy dispersive spectroscopy (EDS) is used to analyze the morphology of both clad layers. The Vickers indentation method is used to determine the hardness values of the clads. The result revealed that the process current in TIG and the exposure time in MHH cladding have a significant effect on the clad layer quality. The average hardness of the TIG clad layer was found to be 1.6 times greater than the MHH processed clad layer. The XRD analysis confirmed the presence of intermetallic phases Ni4W, TiNi, and TiC. The phases TiNi and TiC are responsible for metallurgical bonding in the clad layer.

Keywords: TIG cladding, microwave hybrid heating, nickel alloy, process parameters, microhardness

Financing: The work was carried out within the framework of the state task 0809-2021-0013.

For citation: Gudala S., Konovalov S., Ramesh M.R., Panchenko I. A Comparative study on nickel-based alloy composite claddings prepared by tungsten inert gas and microwave hybrid heating techniques. *Bulletin of the Siberian State Industrial University*. 2023, no. 1 (43), pp. 24–32. *http://doi.org/10.57070/2304-4497-2023-1(43)-24-32*

Original article

СРАВНИТЕЛЬНОЕ ИССЛЕДОВАНИЕ КОМПОЗИТНЫХ ПОКРЫТИЙ НИКЕЛЕВЫХ СПЛАВОВ, ПОЛУЧЕННЫХ ТЕХНОЛОГИЯМИ НАПЛАВКИ С ИСПОЛЬЗОВАНИЕМ ИНЕРТНОГО ГАЗА И МИКРОВОЛНОВОГО ГИБРИДНОГО НАГРЕВА

© 2023 г. С. Гудала[1], С. Коновалов[1], М. Р. Рамеш[2], И. Панченко[1]

[1]**Сибирский государственный индустриальный университет** (Россия, 654007, Кемеровская обл. – Кузбасс, Новокузнецк, ул. Кирова, 42)

[2]**Национальный институт технологий Кантараки** (NH 66, Сриниваснагар, Сураткал, Мангалор, Карнатака, Индия, 575025)

Аннотация. В настоящем исследовании техники наплавки с применением вольфрамового инертного газа (TIG) и гибридного нагрева микроволнами (MHH) использовались для создания толстых слоев покрытия из никелевых сплавов толщиной 1 мм на подложке из титанового сплава 31. При наплавке

TIG ток рассматривали как переменную процесса, тогда как при наплавке МНН в качестве переменной процесса рассматривалось время выдержки. Сканирующая электронная микроскопия (SEM) с энергодисперсионной спектроскопией (EDS) используется для анализа закономерностей структуры обоих плакированных слоев. Для определения твердости используется метод вдавливания по Виккерсу. Результат показал, что технологический ток при TIG и время выдержки при наплавке МНН оказывают значительное влияние на качество плакированного слоя. Было обнаружено, что средняя твердость слоя, покрытого TIG, в 1,6 раза выше, чем слоя, обработанного МНН. Рентгеноструктурный анализ подтвердил наличие интерметаллических фаз Ni_4W, TiNi и TiC. Фазы TiNi и TiC отвечают за металлургическую связь в плакированном слое.

Ключевые слова: ВИГ-наплавка, микроволновый гибридный нагрев, никелевый сплав, технологические параметры, микротвердость

Финансирование: Работа выполнена в рамках государственного задания 0809-2021-0013.

Для цитирования: Гудала С., Коновалов С., Рамеш М.Р., Панченко И. Сравнительное исследование композитных покрытий никелевых сплавов, полученных технологиями наплавки с использованием инертного газа и микроволнового гибридного нагрева // Вестник Сибирского государственного индустриального университета. 2023. № 1 (43). С. 24–32. *http://doi.org/10.57070/2304-4497-2023-1(43)-24-32*

Introduction

Titanium and its alloys are increasingly used in aircraft, marine, and petrochemical industries owing to their high specific strength, good biocompatibility, excellent corrosion, and oxidation resistance. Due to their poor surface hardness and tribological properties the application of titanium alloys is limited [1 – 4]. In this regard, the surface characteristics of the titanium alloy can be improved by surface treatment techniques such as plasma spraying [5], physical vapour deposition [6], and chemical vapour deposition [7] by adding a layer on the surface. Mostly, these techniques improve the surface hardness of the material which enhances the wear resistance. However, some shortcomings such as thin coating or low coating density, and poor substrate-coating adhesion were found in the deposited layers while fabricating with these methods.

Metal matrix composite coatings (MMC) have the potential to use in many industrial applications due to their high hardness, stiffness, and strength. These coatings give more prominent toughness than many single-phase materials [8]. Among several MMC coatings, nickel-based alloys are extensively applied in severe environments because of their good material characteristics. Cooper et al. [9] have studied the nickel-based composite alloy by adding reinforcement particles like WC, TiC and SiC, etc. It is evident from the results that the composite coatings show high hardness and wear resistance even at elevated temperatures. Many studies are preferred tungsten carbide (WC) as a reinforcement material due to its exceptional mechanical properties. P. Farahmand et al. [10] fabricated the nickel-tungsten carbide composite coatings using a diode laser with induction heating and the results showed that the deposited clads attained good porous free and mechanical properties. Farayibi et al. [11] deposited TiC-WC-WC_2 composite coating on titanium alloy using the laser cladding technique and it is evident from the result that the deposited layer hardness is increased by 1.7 times that of titanium alloy. Also, the wear volume of the coating is noted as one-seventh of the wear volume of the substrate. Aytekin and akcin [12] revealed that the composite TIG claddings developed with reinforcement particles in the nickel alloy matrix showed high hardness and corresponding wear resistance. The literature revealed that the applications of several modification techniques are inadequate in the industrial sector, because of technological and economical complications. Yan et al. [13] has demonstrated the fabrication complexity and economical perspective of composite coatings in the study. Patel et al. [14] disclosed the advantage of TIG cladding to attain promising mechanical properties with low equipment and running cost. Even though TIG cladding is a widely accepted surface modification technique, controlling the dilution of the substrate with cladding is quite challenging [15]. Literature suggested that the percentage of dilution is increasing with an increase in current. So, the optimum selection of current for particular cladding material is selected based on a trial and error method. Kaushal et al. [16] deposited the nickel-based alloy clad by microwave hybrid heating technique on the steel and results showed that the microhardness of clad is 3.7 times that of the substrate material. The hardness of the clad is increased due to the formation of the intermetallic compound Ni4W. Dheeraj gupta et al. [17] revealed that WC-12CO clad developed with microwave irradiation has a significant increase in microhardness. Due to the uniform distribution of nano carbides in the clad layer, wear resistance in

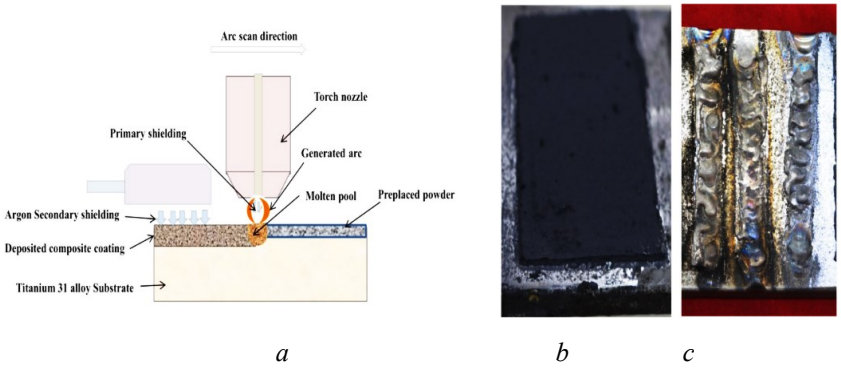

a *b* *c*

Fig. 1. Schematic representation of TIG cladding procedure (*a*), precoated substrate (*b*), deposited clad layers (*c*)
Рис. 1. Схематическое изображение процедуры наплавки TIG (*a*), подложка с предварительно нанесенным покрытием (*b*), нанесенные плакирующие слои (*c*)

creased significantly. In recent years, treating materials with microwave energy has emerged as a rapid processing technique [18]. Microwave energy induces porous free clads with no thermal distortion due to its molecular-level heating.

In the present work, nickel-based alloy clads are developed on titanium 31 alloy substrate material using both tungsten inert gas (TIG) and microwave hybrid heating (MHH) techniques. The effect of current on TIG-deposited cladding and the prominent effect of exposure time in MHH cladding are studied. The comparative study on microstructural and mechanical properties of both TIG and MHH clads is examined.

Methodology

A grade 31 titanium alloy of composition Ti–6Al–3.91V (wt %) with a hardness of 305±10 HV is used as a substrate material procured from Mishra Dhatu Nigam Ltd, India. Before cladding, the plates of dimension (50×50×10 mm) were cut and polished with 400 grit emery papers. The nickel alloy powder (Hoganas Pvt Ltd., Belgium) of chemical composition 47W–7.33Cr–2.21Si–1.91Fe–2.37C–1.61B–bal Ni (wt. %) is selected as a coating material. Before cladding, the powder is mixed with 10 wt. % polyvinyl alcohol (PVA) to make a paste-like substance. Then the powdered paste is evenly applied on the substrate plates with the help of a 1mm metallic mask. Further, precoated samples are kept in the furnace for 1hr at 50 °C to remove moisture content in the coating. It has also enhanced the bonding between coating and substrate.

The TIG cladding is developed with a thoriated tungsten electrode of dimension 2.4 mm. The 3 mm arc length is kept constant. Literature suggested the secondary shielding setup while welding titanium alloys. Argon shrouding gas is used for primary and secondary shielding with a flow rate of 10 l/min and 15 l/min, respectively, to protect the clad from oxidation. It is well known that welding current and scan speed are responsible for energy input in the process. In this study, the scan speed is kept constant, whereas claddings are developed by varying the current. The arc is scanned over the precoated substrate which resulted in the melting of the powder and formed as a clad layer. The schematic diagram of TIG cladding is shown in Fig. 1, *a*. The pre-coated substrate sample is shown in Fig. 1, *b*, and the deposited clad layers at welding currents 80 A, 90 A, and 100 A are shown in Fig. 1, *c*.

In the microwave hybrid heating (MHH) technique, LG domestic microwave of capacity 900 W is utilized. The alumina casket box is developed with pure alumina, and silicon carbide of 10 mm thickness is used as a susceptor. Silicon carbide provides a hybrid heating arrangement and minimizes thermal gradient, which could be used to produce defect-free clads. The graphite sheet is used as a separator to protect the clad layer from contamination with the susceptor. The graphite sheet is placed on the precoated substrate and silicon carbide is positioned on the graphite sheet.

Further, the whole setup is placed on the alumina casket to develop insulation inside the chamber. The MHH schematic setup is shown in Fig. 2, *a*. The deposited clad layer is shown in Fig. 2, *b*. The detailed mechanism of microwave hybrid heating has been explained elsewhere [19 – 21]. The microwave radiation exposure time is varied in a step of 5 minutes. At 5 minute exposure time, powder particles are not fully melted. The powder particles are partially melted at 10 and 15 minute exposure time, but the clad is not properly bonded with the substrate. At 20 minute exposure time, the powder is partially melted is well bonded with the substrate. At the exposure time of 25 minutes, the clad is developed and is metallurgically bonded with the substrate. The TIG and MHH processed clad were sectioned and polished well with a diamond paste. The samples are cleaned with acetone before proceeding with characterizations. The cross-sectional images

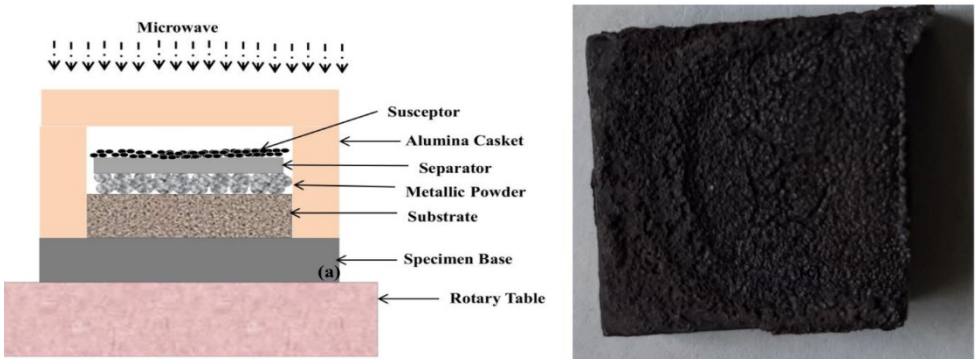

a *b*

Fig. 2. Schematic representation of MHH cladding procedure (*a*), cladded specimen (*b*)
Рис.2. Схематическое изображение процедуры плакирования МНН (*a*), плакированный образец (*b*)

of TIG and microwave treated clads are observed with the scanning electron microscope (SEM) with attached energy dispersive spectra (EDX). The microhardness measurements of the claddings are measured using OMNITECH Vickers microhardness tester with a normal load of 300 g and dwell time of 10 s. The *x*-ray diffraction (XRD) (DX GE-2P, JEOL, Japan) is employed for phase analysis of the deposited clads.

Results and discussion

Fig. 3 and Fig. 4 depict that the TIG and MHH of nickel-based alloy clads are well bonded with the substrate. The claddings deposited with the TIG welding technique showed very well dilution with the substrate. The thickness of the claddings is increasing with an increasing current from 80 A to 100 A. The WC particles in the nickel matrix are well dispersed in the nickel alloy matrix. As increasing current from 80 A to 100 A, WC dissolution is increased. This could happen due to the change in energy input, which further changes the clad layer's solidification rate. It is observed that, due to the dilution of the substrate, cladding thickness is increased with increasing current. The clad layer thickness at 80A is comparatively low (1.1 – 1.2 mm). At a higher current (100 A), clad layer thickness was found in the range of 1.28 – 1.35.

Abundant WC particles are preserved in the upper clad layer responsible for higher average surface hardness (Fig. 3, *a*). Fig 3, *c* shows the more uniform clad layer compared with the clad processed at 80 A (Fig. 3, *a*), which is due to the dissolution of WC particles. However, the chemical composition of the clad layer is changing while increasing the current, which leads to a reduction in hardness. From the SEM images, it is observed that WC particles are collected at the bottom due to their higher density and melting point than nickel alloy. It is also evident that convection current of the weld pool is not sufficient to prevent the WC particles from sinking to the bottom.

However, WC particles near the interface restrict the diffusion of cladding with the substrate. Comparatively, more pores are formed at 80 A current than other processed clads. This could be due to the inadequate heat input which causes entrapment of Ar shielding gas in the clad. No crack is formed at the interface, and clads are metallurgically bonded with the substrate at all processing conditions. Fig. 5 represents the magnified cross-sectional images of TIG clad deposited at 80 A current. It can be seen that Ni alloy-WC clad is metallurgically bonded with the substrate. Fig. 6 shows the EDS analysis performed on the selected area deposited at welding current 80 A.

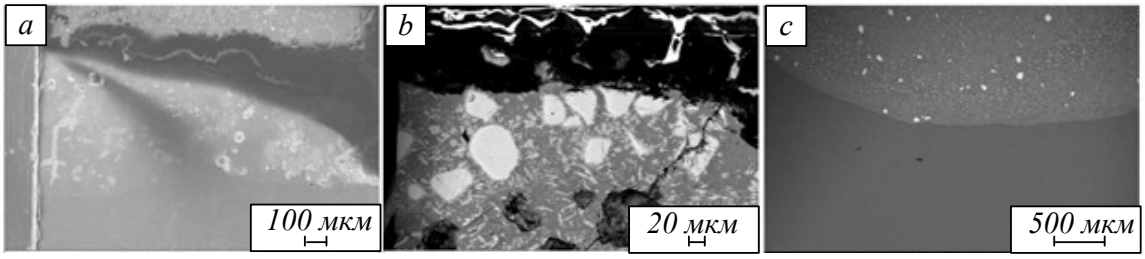

Fig. 3. SEM images of nickel alloy cladding cross section produced by TIG cladding method with processing current of 80 A (*a*), 90 A (*b*), 100 A (*c*)
Рис. 3. СЭМ-изображения поперечного сечения покрытия из никелевого сплава, полученного методом TIG-наплавки при токе обработки 80 А (*a*), 90 А (*b*), 100 А (*c*)

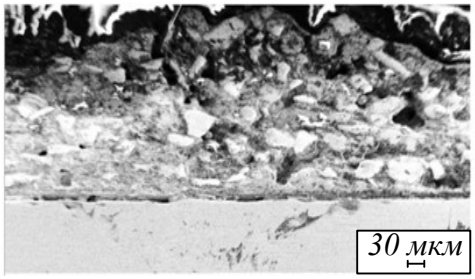

Fig. 4. Cross sectional SEM image of nickel alloy clad produced by MHH cladding method
Рис. 4. СЭМ-изображение поперечного сечения, плакированного никелевым сплавом, полученного методом плакирования МНН

Near the interface, interdendritic eutectic precipitations are found, as can be seen in Fig. 7, *a*. The irregular blocks found in the compound are rich in W and C. To identify the elemental distribution in the cladding, EDS analysis is conducted. Fig. 7, *a* shows blocky white shaded particles (*B*), and grey shaded particles (*C*) marked in the TIG clad layer processed at 80 A primarily containing W and C and W and Ni, respectively. The dendritic structures formed on the substrate growing towards the clad layer. These dendritic structures at the interface (*C*) are rich in titanium and nickel, and the matrix (*D*) is containing nickel alloy (Fig. 7, *b*). Fig. 7 shows SEM image of the MHH deposited clad layer. It is revealed that approximately 1±50mm crack-free clad is deposited.

In the clad layer, WC particles directly interact with the microwaves due to their higher skin depth. Then, the heat conduction from WC particles further raises the temperature of nickel alloy particles. After reaching critical temperature, the whole powder particles start interacting with the microwaves, which leads to the melting of powder particles. The observations are noted in a step of 5-minute microwave exposure time. At the 25 minutes exposure time, the microwave radiation is enough to melt the preplaced power layer, which further melts the thin layer of the substrate material. Due to this, the clad layer is partially diffused with the titanium substrate. The partially melted substrate can be seen in Fig. 7, *a*. Few pores are formed in the clad layer, which may be due to the exothermic reactions of the powders. It is observed that WC particles in the nickel alloy matrix are well distributed. The irregular WC particles are partially dissolved in the clad layer. To identify the elemental distribution in the clad layer, EDS study is conducted. The EDS study confirmed that marks *A* and *C* in Fig. 7, *a* are identified as WC and nickel alloy matrix, respectively. The interface zone (*B*) is rich in titanium and nickel alloy, which is maybe due to the partial melting of the substrate material. The dissolution of WC particles is observed in the clad layer. Due to this, the surrounded nickel alloy matrix contains little W and C. The EDS analysis shows the presence of possible intermetallic phases in the clad layer.

The microhardness profiles of the claddings produced by TIG and MHH processes at different process conditions are evaluated by considering the number of readings along the clad depth. Fig. 8 and Fig. 9 show the Vickers microhardness distributions of the TIG clad and MHH clad along with the depth, respectively. It is to be noted that hardness values along the cross-section are not uniform. The results show that the hardness of the clad is increasing while moving away from the substrate. The addition of WC particles in the matrix influences the formation of hard phases within the nickel alloy matrix. The sudden increase in microhardness value in the graph indicates WC particle distribution in the clad. The higher hardness indicates the rapid cooling rate of the clad during the development of the cladding.

Moreover, due to the rapid cooling of the molten zone, WC particles are not dissolved fully in the matrix. The comparison results of hardness profiles are showing that TIG processed clad deposited at a lower current (80 A) has higher average microhardness. Besides, at higher energy input, WC is fully melted and dissolved in the matrix. Besides, the

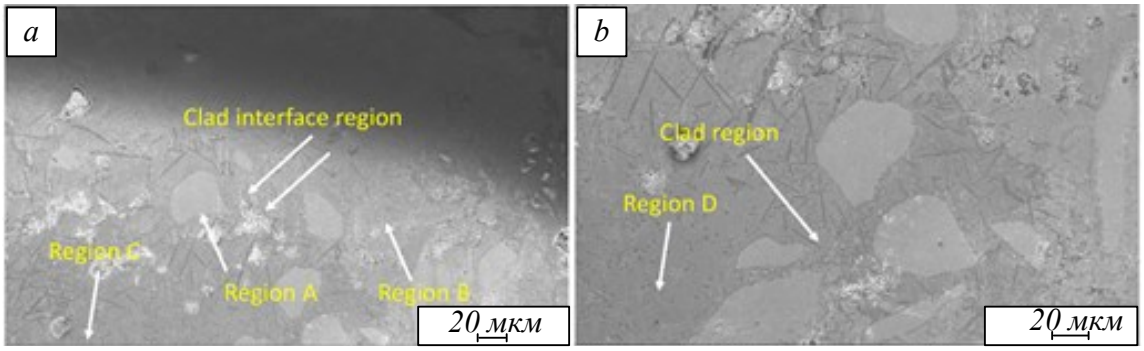

Fig. 5. Magnified SEM image of TIG clad processed at 80 A (*a*), Clad-interface region (*b*) clad layer
Рис. 5. Увеличенное СЭМ-изображение TIG-плакировки, обработанной при 80 А области поверхности плакирования (*a*), и плакированный слой (*b*)

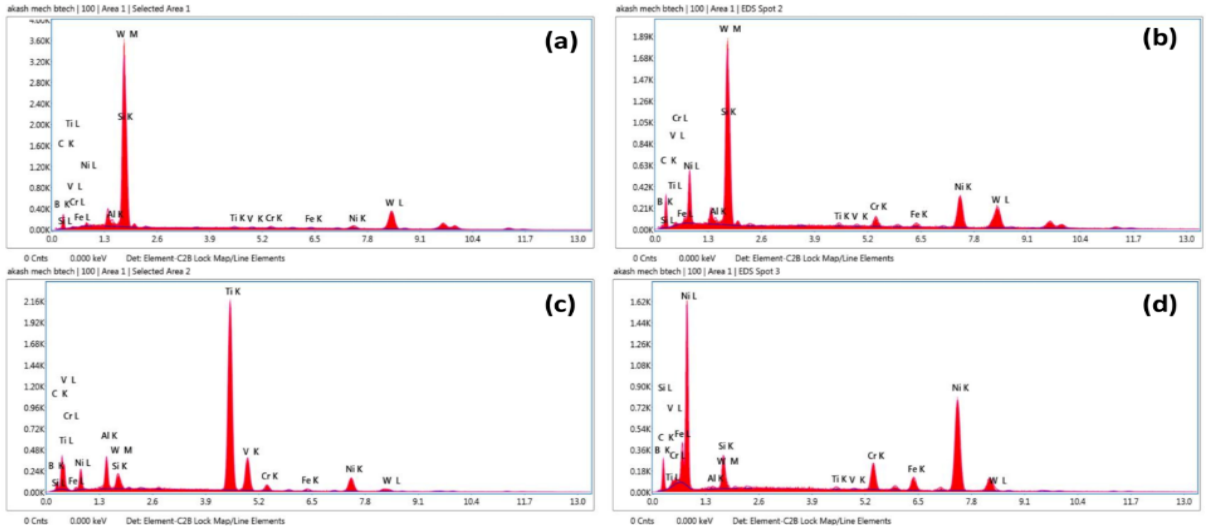

Fig. 6. Typical EDS spectra of: (*a*) region *A*, (*b*) region *B*, (*c*) region *C*, (*d*) region *d*
Рис. 6. Типичные спектры ЭДС:
a – область *A*; *b* – область *B*; *c* – область *C*; *d* – область *Д*

change in chemical composition at the current 100 A due to higher dilution causes the hardness value reduction. A sudden increase in hardness value is observed due to the collected WC particles near the interface. Also, the MHH clad hardness is deviating along the cross-section. The hardness of the MHH clad mainly depends on the energy input and exposure time. The claddings deposited by TIG and MHH deposited clads are 3.5 and 2 times higher than the titanium alloy substrate, respectively, attributed to the formation of hard phases like $Cr_{23}C_6$, WC, W_2C, Ni_4W, and TiC. From Fig. 8 and Fig. 9, it can be seen that the average hardness values of the TIG and MHH processed clads are 965.5274 and 591.319, respectively. It is observed that the hardness value of the TIG deposited clad is 1.6 times the hardness value of the MHH clad. In the interface zone, TIG deposited clad having hardness value 320 – 550. Whereas MHH clad is having hardness around 320 – 415. Also, HAZ near the interface in both clad shows more hardness than the reference titanium substrate. The overall hardness values of the claddings are mostly dependent on the energy input and reinforcement volume in the clad. It is worth noting that microhardness studies of TIG and MHH claddings can evaluate the respective wear performances approximately. Fig. 10, and Fig. 11 show the XRD analysis of nickel-based alloy clad deposited by both TIG and MHH cladding, respectively. The XRD patterns of both TIG and MHH treated clad show a similar sequence of peaks formation. The phases TiC and TINi formed in the TIG cladding might be due to the dilution of substrate material in the clad. Due to the high

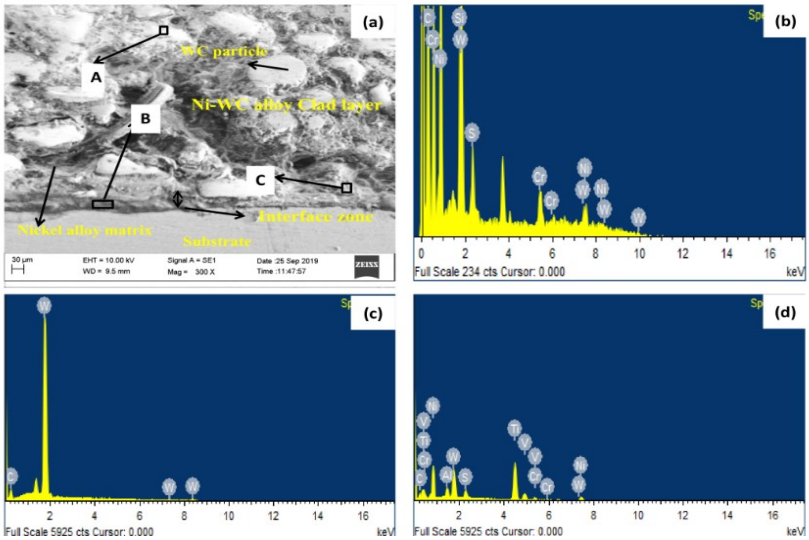

Fig. 7. Typical EDS spectra of: (*a*) region *A*, (*b*) region *B*, (*c*) region *C*, (*d*) region *d*
Рис. 7. Увеличенное СЭМ-изображение в оболочке МНН (*a*) и спектры ЭДС области *A* (*b*), области *B* (*c*), области *C* (*d*)

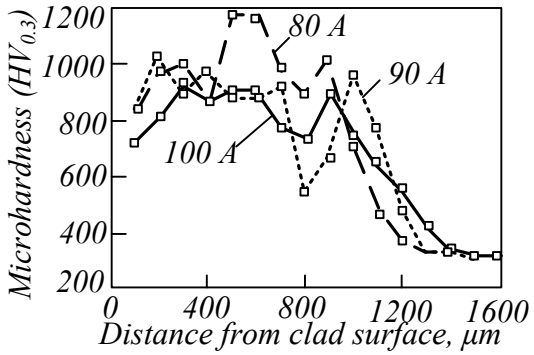

Fig. 8. Hardness distribution of TIG clad cross section along the depth at different processing current
Рис. 8. Распределение твердости поперечного сечения TIG-наплавки по глубине при различном токе обработки

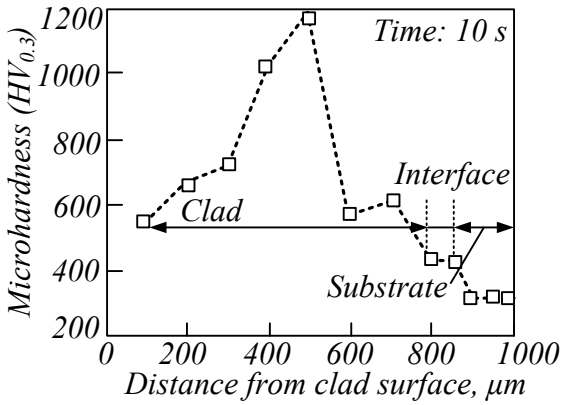

Fig. 9. Hardness distribution of MHH clad cross section along the depth at 25 minute exposure time
Рис. 9. Распределение твердости поперечного сечения наплавки МНН по глубине при времени выдержки 25 минут

temperature in the clad, WC particles are dissolved and formed as the W_2C phase. The W_2C phase is less in the MHH deposited clad than the TIG process due to comparatively lesser energy input causing lesser dissolution of WC particles. The intermetallic phase Ni_4W is formed in the clad layer might be due to the nickel alloy matrix interaction with the free-W. The TIG and MHH treated clad have typical phases such as Ni_4W, WC, W_2C, $Cr_{23}C_6$, Cr_3Si, Cr_7C_3, and TiNi. The MHH clad was processed at a 25 minute exposure time having TiNi phase, which is attributed to the diffusion of substrate material in the clad.

Conclusions

The nickel alloy-tungsten carbide 1 mm thick composite claddings are effectively deposited on titanium 31 alloy using TIG and MHH cladding techniques. The main conclusions can be summarized as follows.

The TIG and MHH deposited claddings have an excellent metallurgical bond on the interface, and no cracks were observed along the clad cross-section. Comparatively, fewer pores are observed in the MHH clad layer than TIG processed clad layer.

The average hardness of the TIG clad layer is 3.5, and the MHH clad is 2 times the titanium alloy. The dissolution of tungsten carbide particles in the nickel matrix is attributed to the amount of energy input, further influencing the hardness of the clad layer.

The TIG deposited clad layer hardness is decreasing as an increasing TIG current from 80 A to 100 A. It is observed that the TIG clad layer thickness is increasing from 1.21 mm to 1.50 mm as the current increases from 80 A to 100 A. The phases TiNi and TiC formed in the TIG cladding indicate the dilution of the substrate with the clad.

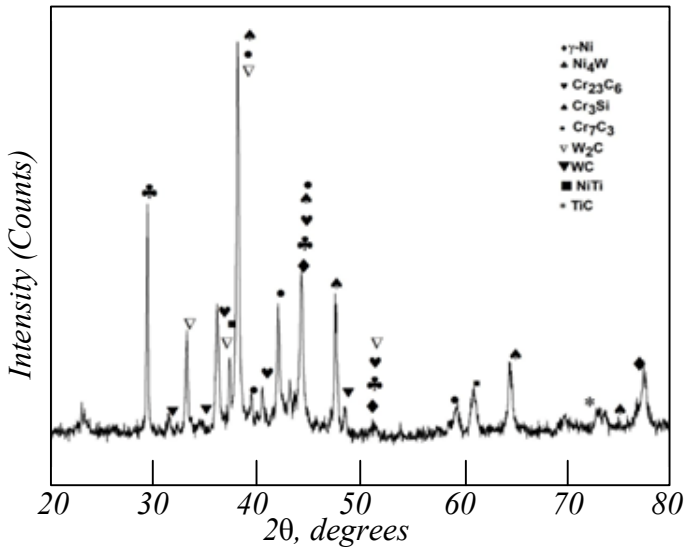

Fig. 10. XRD spectra of TIG clad layer processed at 80 A
Рис. 10. Рентгенодифракционные спектры плакирующего слоя TIG, обработанного при 80 А

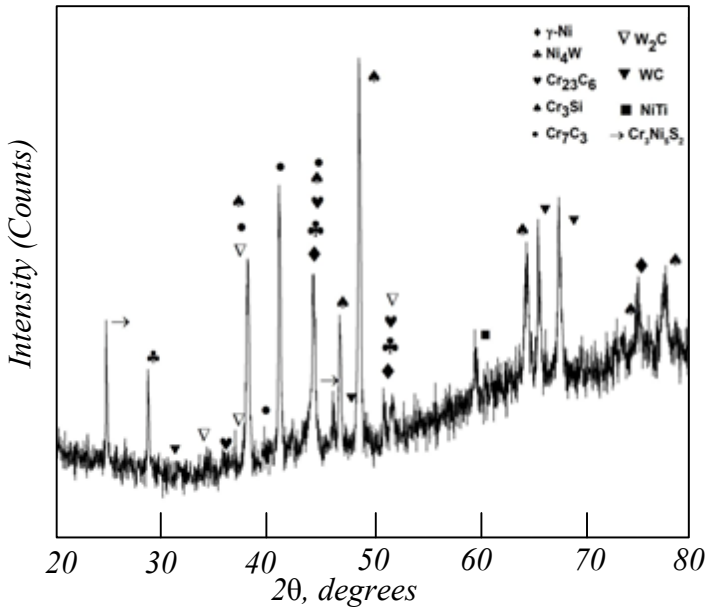

Fig. 11. XRD spectra of MHH clad layer processed at 25 minutes exposure time
Рис. 11. Спектры РФА обработанного плакирующего слоя МНН при времени экспозиции 25 мин

In the MHH cladding, microwave radiation of 25 minutes of exposure time is sufficient to melt the preplaced nickel alloy-tungsten carbide clad layer. The tungsten carbide particles are finely dispersed in the nickel alloy matrix clad. The nickel alloy matrix is enriched in W and C because of the partial dissolution of WC particles. The TiNi phase is formed in the MHH clad attributed to the mutual diffusion of the substrate and the clad.

REFERENCES

1. Courant B., Hantzpergue J.J., Benayoun S. Surface treatment of titanium by laser irradiation to improve resistance to dry-sliding friction. *Wear.* 1999, vol. 236, pp. 39–46. *https://doi.org/10.1016/S0043-1648(99)00254-9*
2. Wang H.M., Liu Y.F. Microstructure and wear resistance of laser clad Ti_5Si_3/$NiTi_2$ intermetallic composite coating on titanium alloy. *Materials Science and Engineering.* 2002, vol. 338, pp. 126–32. *https://doi.org/10.1016/j.surfcoat.2022.128727*
3. Altus E., Konstantino E. Optimum laser surface treatment of fatigue damaged Ti–6Al–4V alloy. *Materials Science and Engineering*. 2001, vol. 302, pp. 5. *https://doi.org/10.1016/S0921-5093(00)01360-5*
4. Bruni S., Martinesi M., Stio M., Treves C., Bacci T., Borgioli F. Effects of surface treatment of Ti–6Al–4V titanium alloy on biocompatibility in cultured human umbilical vein endothelial cells. *Acta biomaterialia*. 2005, vol. 1, pp. 223–234. *https://doi.org/10.1016/j.actbio.2004.11.001*
5. Wang W.M., Yang B., Du L.Z., Zhang W.G. Diffusion research between Ni_3Al coating and titanium alloy produced by plasma spraying process. *Applied surface science*. 2010, vol. 256, pp. 3342–3345. *https://doi.org/10.1016/j.apsusc.2009.12.031*
6. Costa M.Y.P., Venditti M.L.R., Cioffi M.O.H., Voorwald H.J.C., Guimarães V.A., Ruas R. Fatigue behavior of PVD coated Ti–6Al–4V alloy. *International journal of fatigue.* 2011, vol. 33, pp. 759–765. *https://doi.org/10.1016/j.ijfatigue.2010.11.007*
7. Zhu Y.H., Wang W., Jia X.Y., Akasaka T., Liao S.S., Watari F. Deposition of TiC film on titanium for abrasion resistant implant material by ion-enhanced triode plasma CVD. *Applied surface science.* 2012, vol. 262, pp. 156–158. *https://doi.org/10.1016/j.apsusc.2012.03.152*
8. Emamian A., Corbin S.F., Khajepour A. Tribology characteristics of in-situ laser deposition of Fe–TiC. *Surface coatings and technology*. 2012, vol. 206, pp. 4495–4501. *http://doi.org/10.1016/j.surfcoat.2012.01.051*
9. Cooper D.E., Blundell N., Maggs S., Gibbons G.J. Additive layer manufacture of Inconel625 metal matrix composites, reinforcement material evaluation. *Journal of Materials processing technology.* 2013, pp. 2191–2200, *https://doi.org/10.1016/j.jmatprotec.2013.06.021*
10. Farahmand P. Laser cladding assisted by induction heating of Ni–WC composite enhanced by nano-WC and La_2O_3. *Ceramics International.* 2014, vol. 40, pp. 15421–15438. *https://doi.org/10.1016/j.ceramint.2014.06.097*
11. Farayibi P.K., Folkes J., Clare A., Oyelola O. Cladding of pre-blended Ti–6Al–4V and WC powder for wear resistant applications. *Surface*

and coatings technology. 2011, vol. 206, pp. 372–377. *https://doi.org/10.1016/j.surfcoat.2011.07.033*

12. Aytekin H., Akcin Y., Characterization of borided Incoloy 825 alloy. *Materials & Design*. 2013, vol. 50, pp. 515–521. *https://doi.org/10.1016/j.matdes.2013.03.015*

13. Yan H., Zhang P., Yu Z., Lu Q., Yang S., Li C. Microstructure and tribological properties of laser-clad Ni–Cr/TiB_2 composite coatings on copper with the addition of CaF_2. *Surface coatings and technology*. 2012, vol. 206, pp. 404. *http://doi.org/10.1016/j.surfcoat.2012.03.086*

14. Patel P., Mridha S., Baker T.N. Influence of shielding gases on preheat produced in surface coatings incorporating SiC particulates into microalloy steel using TIG technique. *Materials science and technology*. 2014, vol. 30, pp. 1506–1514. *http://doi.org/10.1179/1743284713Y.0000000481*

15. Chakraborty G., Kumar N., Das C.R., Albert S.K., Bhaduri A.K., Dash S. Study on microstructure and wear properties of different nickel base hardfacing alloys deposited on austenitic stainless steel. *Surface and coatings technology*. 2014, vol. 244, pp. 180–188. *http://dx.doi.org/10.1016/j.surfcoat.2014.02.013*

16. Kaushal S., Gupta D., Bhowmick H. On processing of Ni-WC based functionally graded composite clads through microwave heating. *Materials and Manufacturing processes*. 2018, vol. 33, pp. 822–828. *https://doi.org/10.1080/10426914.2017.1401724*

17. Gupta D., Sharma A.K. Development and microstructural characterization of microwave cladding on austenitic stainless steel. *Surface coatings and technology*. 2011, vol. 205, pp. 5147–5155. *https://doi.org/10.1016/j. surfcoat.2011.05.018*

18. Gupta D., Sharma A.K. Microwave cladding: a new approach in surface engineering. *Journal of manufacturing processes*. 2014, vol. 16, pp. 176–82. *https://doi.org/10.1016/j.jmapro.2014.01.001*

19. Zafar S., Sharma A.K., Development and characterisations of WC–12Co microwave clad. *Materials characterization*. 2014, vol. 96, pp. 241–248. *https://doi.org/10.1016/j.matchar.2014.08.015*

20. Gupta D., Sharma A.K., Investigation on sliding wear performance of WC10Co2Ni cladding developed through microwave irradiation. *Wear*. 2011, vol. 271, pp. 1642–50. *https://doi.org/10.1016/j.wear.2010.12.037*

21. Gupta D., Sharma A.K. Microstructural characterization of cermet cladding developed through microwave irradiation. *Journal of materials engineering and performance*. 2012, vol. 21, pp. 2165–2172. *https://doi.org/10.1007/s11665-012-0142-2*

Information about the authors

S. Gudala, *PhD., Senior Researcher Fellow,* Siberian State Industrial University
ORCID*:* 0000-0003-0405-5829
E-mail*:* gsuresham@gmail.com

Sergey V. Konovalov*, Dr. Sci. (Eng.), Prof., Vice-Rector for Research and Innovation,* Siberian State Industrial University
ORCID*:* 0000-0003-4809-8660
E-mail*:* konovalov@sibsiu.ru

M.R. Ramesh, National Institute of Technology Karnataka
ORCID*:* 0000-0003-2280-1995
E-mail: gsuresham@gmail.com

Irina A. Panchenko*, Cand. Sci. (Eng.), Chief of Laboratory of Electron Microscopy and Image Processing,* Siberian State Industrial University
ORCID: 0000-0002-1631-9644
E-mail: i.r.i.ss@yandex.ru

Сведения об авторах

С. Гудала, *PhD, старший научный сотрудник*, Сибирский государственный индустриальный университет
ORCID*:* 0000-0003-0405-5829
E-mail*:* gsuresham@gmail.com

Сергей Валерьевич Коновалов*, д.т.н., профессор, проректор на научной и инновационной деятельности,* Сибирский государственный индустриальный университет
ORCID*:* 0000-0003-4809-8660
E-mail*:* konovalov@sibsiu.ru

М.Р. Рамеш, *PhD,* Национальный институт технологий Кантараки
ORCID*:* 0000-0003-2280-1995
E-mail: gsuresham@gmail.com

Ирина Алексеевна Панченко**,** *к.т.н., заведующий лабораторией электронной микроскопии и обработки изображений,* Сибирский государственный индустриальный университет
ORCID: 0000-0002-1631-9644
E-mail: i.r.i.ss@yandex.ru

Поступила в редакцию 01.03.2023
После доработки 06.03.2023
Принята к публикации 11.03.2023

Received 01.03.2023
Revised 06.03.2023
Accepted 11.03.2023